

## Electronic Supplementary Information

# Kinetically Stabilized Alivalent Europium-Doped Magnesium Oxide as UV Sensitized Phosphor

Chandresh Kumar Rastogi<sup>a</sup>, SulaySaha<sup>b</sup>, Sri Sivakumar<sup>a,b,c\*</sup>, Raj Ganesh S Pala<sup>b\*</sup> and Jitendra Kumar<sup>a\*</sup>

<sup>a</sup>Materials Science Programme, Indian Institute of Technology Kanpur, 208016, Kanpur, India

<sup>b</sup>Department of Chemical Engineering, Indian Institute of Technology Kanpur, 208016, Kanpur, India

<sup>c</sup>Centre for Environmental Science and Engineering, Indian Institute of Technology Kanpur, 208016, Kanpur, India

Fax: 91-512-2590104; Tel: 91-512-2596143; E-mail: [srisiva@iitk.ac.in](mailto:srisiva@iitk.ac.in), [rpala@iitk.ac.in](mailto:rpala@iitk.ac.in), [jk@iitk.ac.in](mailto:jk@iitk.ac.in)

### Materials Characterization

Thermogravimetry (TG) analysis of the sol-gel product was undertaken to ascertain calcination condition of oxide formation. An X-ray diffractometer (X' Pert PRO), an UV-Vis-NIR spectrophotometer (Varian model Carry 5000), a transmission electron microscope (FEI Technai G2), high resolution transmission electron microscope (Ultra High Resolution FEG TEM JEOL-JEM 2010) and an X-ray fluorescence spectrometer (Rigaku ZSX Primus series) were used for evaluation of phase(s), optical absorption measurements, microstructure, and composition analysis, respectively. A Fourier transform infrared (FTIR) spectrometer (BRUKER vertex-70) was utilized to identify various stretching bonds present in samples. Further, a fluorescence spectrophotometer (Edinburgh instruments FLSP 920), equipped with double monochromator, 450 W Xenon lamp as excitation source, and Peltier element cooled Hamamatsu R928-P PMT detector, was employed for obtaining the luminescence spectra. The luminescence lifetime was estimated by recording the decay curve using a 100W micro flash lamp ( $\mu$ F920H) as the excitation source.

### Thermogravimetric Analysis

In order to find out the calcination temperature, thermogravimetry (TG) analysis of dried sol-gel product (magnesium oxalate dihydrate) has been carried out by heating in air at the rate of 4 °C/min and monitoring the change in weight as a function of temperature. The weight vs.

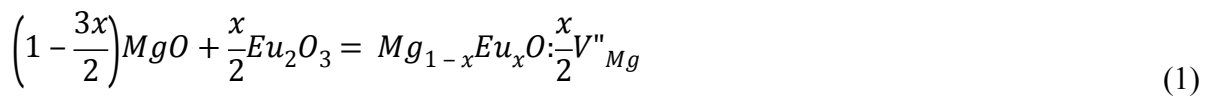
temperature plot indicates two stages of weight loss (Fig. 1 of ESI). In the first stage, weight loss of 28.7% occurs over a range of 172–270 °C due to removal of crystalline water present in magnesium oxalate dihydrate. In the second stage, weight loss of 43.4% observed in the range 375–495 °C corresponds to thermal decomposition of anhydrous magnesium oxalate to magnesium oxide. As no weight loss was observed beyond 495 °C, MgO was prepared by decomposition of magnesium oxalate dihydrate at ~500 °C. The calcination temperature for the samples  $Mg_{1-x}Eu_xO:(x/2)V''_{Mg}$  ( $x=0-0.10$ ) was chosen as 500 °C.

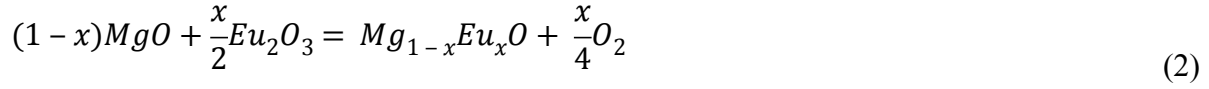
## Computational Methods

Density functional theory (DFT) calculations have been performed to obtain trends in stability  $Mg_{1-x}Eu_xO:(x/2)V''_{Mg}$ , MgO and europium oxides. The calculations were performed with and without vacancy in  $Mg_{1-x}Eu_xO:(x/2)V''_{Mg}$ . The calculations have been performed with plane-wave basis set (energy cut-off of 400 eV) and projector-augmented method<sup>1</sup> using Perdew, Burke and Ernzerhof (PBE) exchange-correlation functional<sup>2</sup> as implemented in *Vienna Ab initio Simulation Package* (VASP) software.<sup>3,4</sup> The pseudo-potential of Mg, O and Eu contain 2, 6 and 17 valence electrons. The Brillouin zone is sampled using a gamma centered mesh of k-points (8×8×8) for single cell calculation of oxides of europium and magnesium. For rest of the super cells calculations involving point defects, a gamma centered mesh of k-points are used which are adjusted according to the supercell length. The geometry has been relaxed by optimizing all structural parameters until the forces on each ion are smaller than 0.01 eV/Å. To correlate the ionic state of dopant, atomic charges have been estimated by the Bader decomposition scheme.<sup>5</sup>

After relaxation, the bulk lattice constant of MgO and  $Eu_2O_3$  are found to be 4.24 Å and 11.08 Å respectively as against 4.21 Å (JCPDS PDF No. 04-0829) and 10.86 Å (JCPDS PDF No. 34-0392) reported in the literature.

The explicit reactions describing the solid state formation for the different europium concentration used in the present study are:





We have carried out the stability analysis with respect to  $Eu_2O_3$  rather than  $EuO$  as in the present study experimentally we have found that phase segregation occurs through  $Eu_2O_3$ . Equation 1 corresponds to trivalent europium doping in  $MgO$  with creation of cationic vacancy whereas Equation 2 corresponds to doping of divalent europium without any vacancy formation (assuming the decomposed doped oxides forms  $Eu_2O_3$ ). In order to determine the relative stability of the divalent  $Eu$ -doped with trivalent  $Eu$ -doped  $MgO$  structures, where the introduction of an increasing number of cation vacancies corresponds to an increase of the oxidation state. The heat of formation,  $\Delta E^f$  corresponding to the different doping concentration for above four cases is evaluated using following equations:

$$\Delta E_{Mg_{1-x}Eu_xO:(x/2)V''_{Mg}}^f = E_{Mg_{1-x}Eu_xO:(x/2)V''_{Mg}} - (1 - \frac{3x}{2})E_{MgO} - \frac{x}{2}E_{Eu_2O_3} \quad (3)$$

$$\Delta E_{Mg_{1-x}Eu_xO}^f = E_{Mg_{1-x}Eu_xO} - (1-x)E_{MgO} + \frac{x}{4}E_{O_2} - \frac{x}{2}E_{Eu_2O_3} \quad (4)$$

Where  $Mg_{1-x}Eu_xO:(x/2)V''_{Mg}$  and  $E_{Mg_{1-x}Eu_xO}$  are the energies of the systems with cationic vacancy and without cationic vacancy, respectively.

Table S1. Elemental composition obtained from energy dispersive x-ray analysis of  $\text{Mg}_{1-x}\text{Eu}_x\text{O}:(x/2)\text{V}''_{\text{Mg}}(x=0.005)$  samples

<b>Element</b>	<b>Weight%</b>	<b>Atomic%</b>
<b>O K</b>	<b>49.95</b>	<b>62.51</b>
<b>Mg K</b>	<b>25.43</b>	<b>20.94</b>
<b>Si K</b>	<b>22.90</b>	<b>16.32</b>
<b>Eu L</b>	<b>1.72</b>	<b>0.23</b>
<b>Totals</b>	<b>100.00</b>	

Table S2. Component of lifetime after double exponential fitting for Mg<sub>1-x</sub>Eu<sub>x</sub>O:(x/2)V<sup>''</sup><sub>Mg</sub>(x=0.005 and 0.01) samples

Sl. No.	Composition (x)	$\tau_1(\mu\text{s})$	$\tau_2(\mu\text{s})$	A <sub>1</sub> (%)	A <sub>2</sub> (%)	$\chi^2$
1	0.005	586	2174	51.67	48.33	1.52
2	0.01	519	2105	74.22	25.78	1.56

Table S3: Comparison of phonon energy of oxide matrices and effective lifetime of  $\text{Eu}^{3+}$  ions

S.No.	Host for $\text{Eu}^{3+}$ matrix	Effective lifetime (ms)	Phonon energy ( $\text{cm}^{-1}$ )	Reference
1	$\text{Y}_2\text{O}_3$	2.0 <sup>6</sup>	600 <sup>7</sup>	Myint <i>et al.</i> , <sup>6</sup> Vetrone <i>et al.</i> <sup>7</sup>
2	$\text{Gd}_2\text{O}_3$	1.75 <sup>8</sup>	600 <sup>9</sup>	Debasuet <i>al.</i> , <sup>8</sup> Guo <i>et al.</i> <sup>9</sup>
3	ZnO	1.25 <sup>10</sup>	574 <sup>11</sup>	Liu <i>et al.</i> , <sup>10</sup> Fonoberov <i>et al.</i> <sup>11</sup>
4	$\text{Lu}_2\text{O}_3$	1.33 <sup>12</sup>	600	Yang <i>et al.</i> , <sup>12</sup> Vetrone <i>et al.</i> <sup>7</sup>
5	MgO	0.216 <sup>13</sup>	750	Penget <i>al.</i> <sup>13</sup>
<b>6</b>	<b>MgO</b>	<b>1.80</b>	<b>750</b>	<b>MgO matrix in the present work</b>

Table S4: Estimated luminescence lifetime of  $^5D$  level and quantum yield for  $Mg_{1-x}Eu_xO:(x/2)V''_{Mg}(x)$  samples

<b>S. No.</b>	<b>Composition (x)</b>	<b>Lifetime (ms)</b>	<b>Quantum yield (%)</b>
1	0.1	0.72	24.8
2	0.5	1.81	62.4
3	1	0.9	31.0
4	5	0.8	27.6
5	10	0.41	14.1

Table S5. Heat of formation for  $\text{Mg}_{1-x}\text{Eu}_x\text{O}:(x/2)\text{V}''_{\text{Mg}}$  systems

<b>Composition (x)</b>	<b>Heat of formation (with vacancy)(eV)</b>	<b>Heat of formation(without vacancy)(eV)</b>
0.0625	3.7	7.8
0.0417	3.6	7.7
0.0312	3.5	7.5
0.0156	3.2	7.4

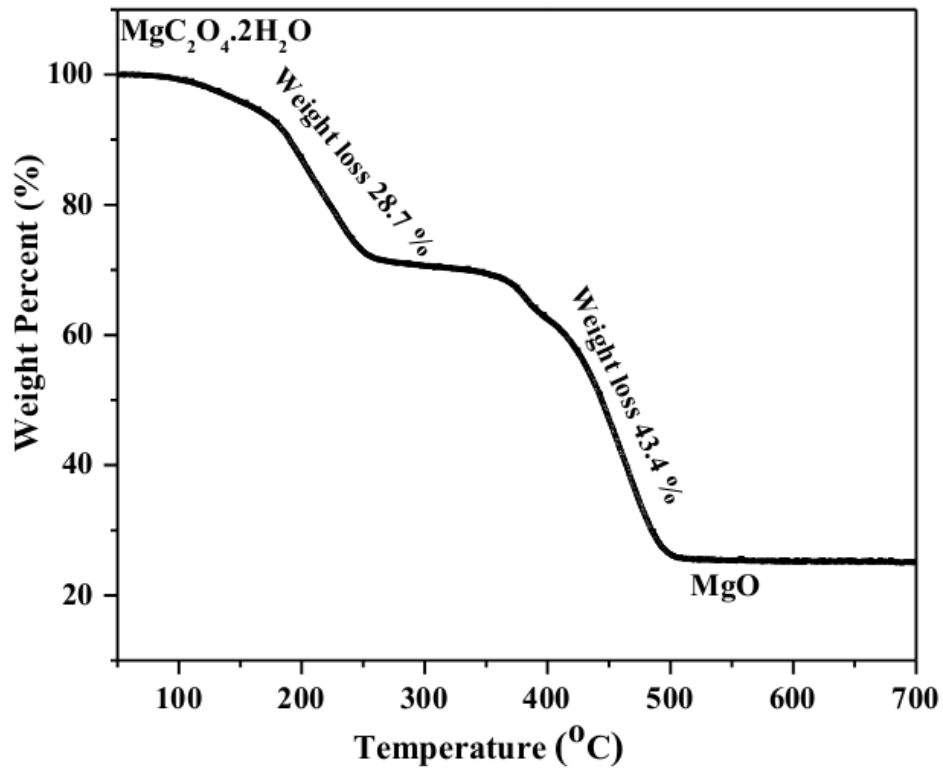


Fig.S1 TGA plot of dried magnesium oxalate dihydrate ( $\text{MgC}_2\text{O}_4 \cdot 2\text{H}_2\text{O}$ ) powder

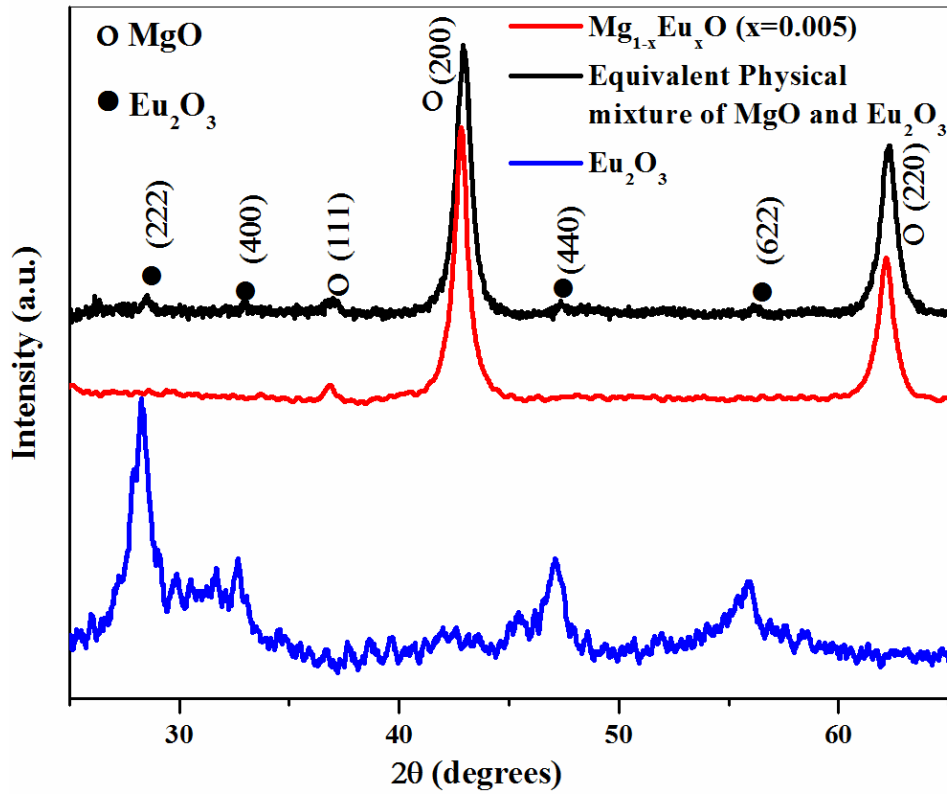


Fig.S2 X-ray diffraction patterns of (a)  $\text{Mg}_{1-x}\text{Eu}_x\text{O}:(x/2)\text{V}''_{\text{Mg}}$  ( $x=0.005$ ) sample (b) Physically mixed MgO and  $\text{Eu}_2\text{O}_3$  corresponding to  $x=0.005$

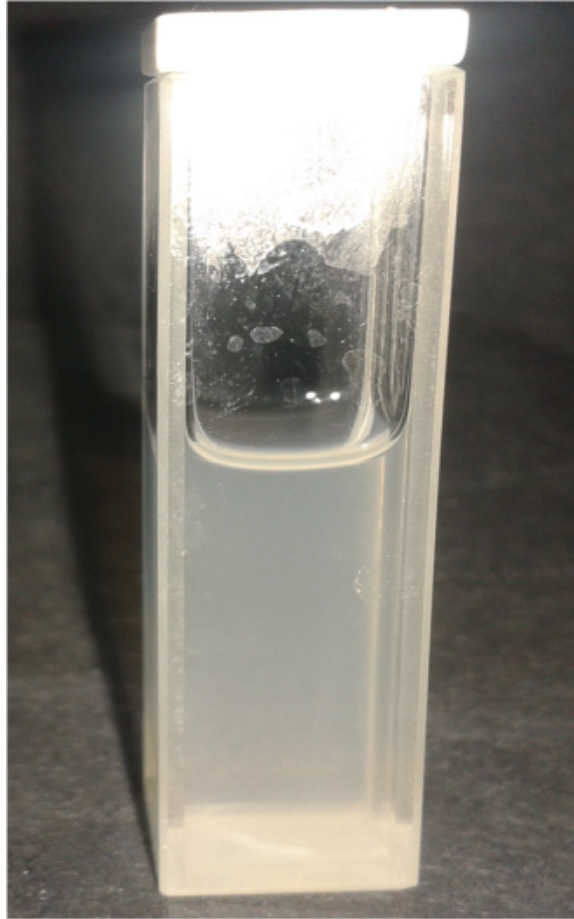


Fig.S3 Digital photograph showing the dispersion of  $\text{Mg}_{1-x}\text{Eu}_x\text{O}:(x/2)\text{V}''_{\text{Mg}}$  ( $x=0.005$ ) particles in ethanol. The concentration of the solution taken is 2.5 mg/mL

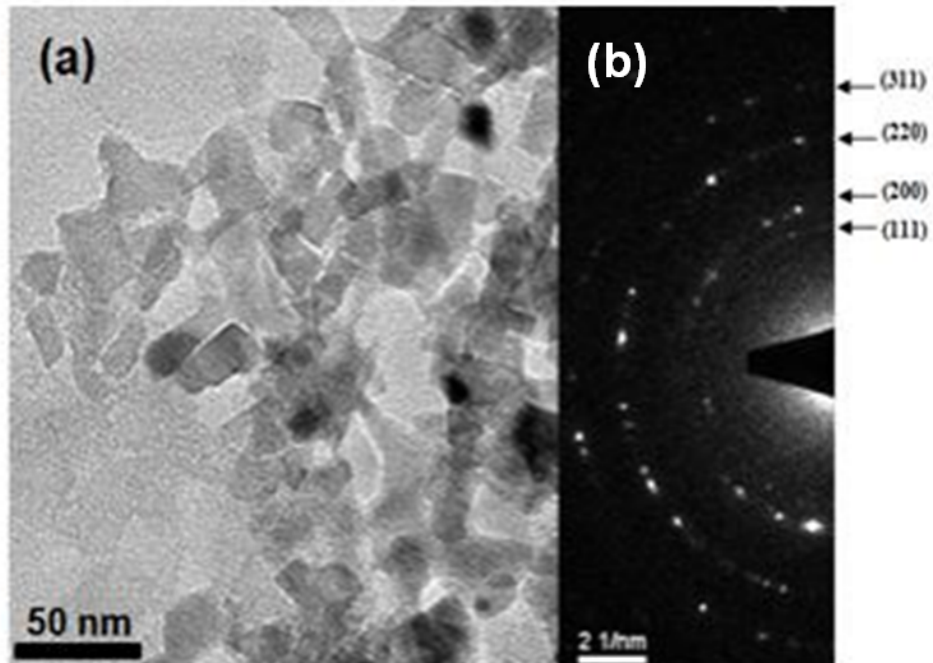


Fig.S4(a) Transmission electron micrograph and (b) corresponding selected area electron diffraction (SAED) pattern of undopedMgO sample

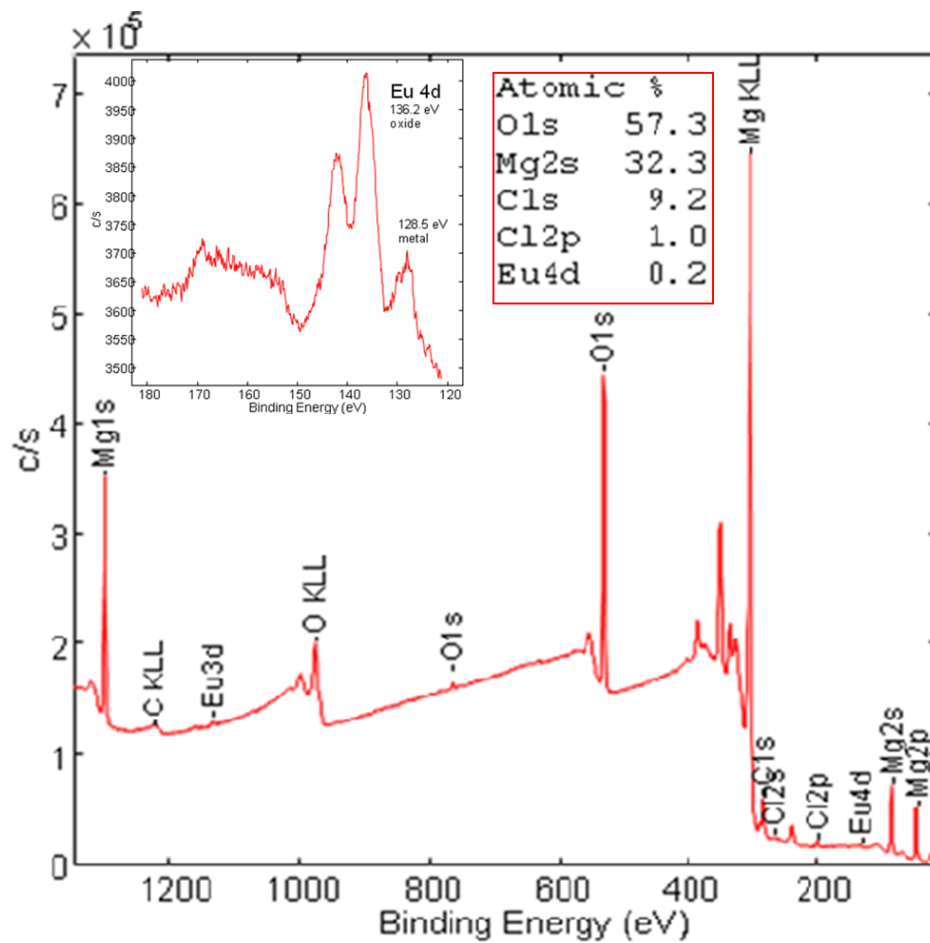


Fig. S5X-ray photoelectron spectrum (with inset corresponding to spectrum recorded in energy range 120-190 eV) of  $\text{Mg}_{1-x}\text{Eu}_x\text{O}:(x/2)\text{V}''_{\text{Mg}}(x=0.01)$  samples

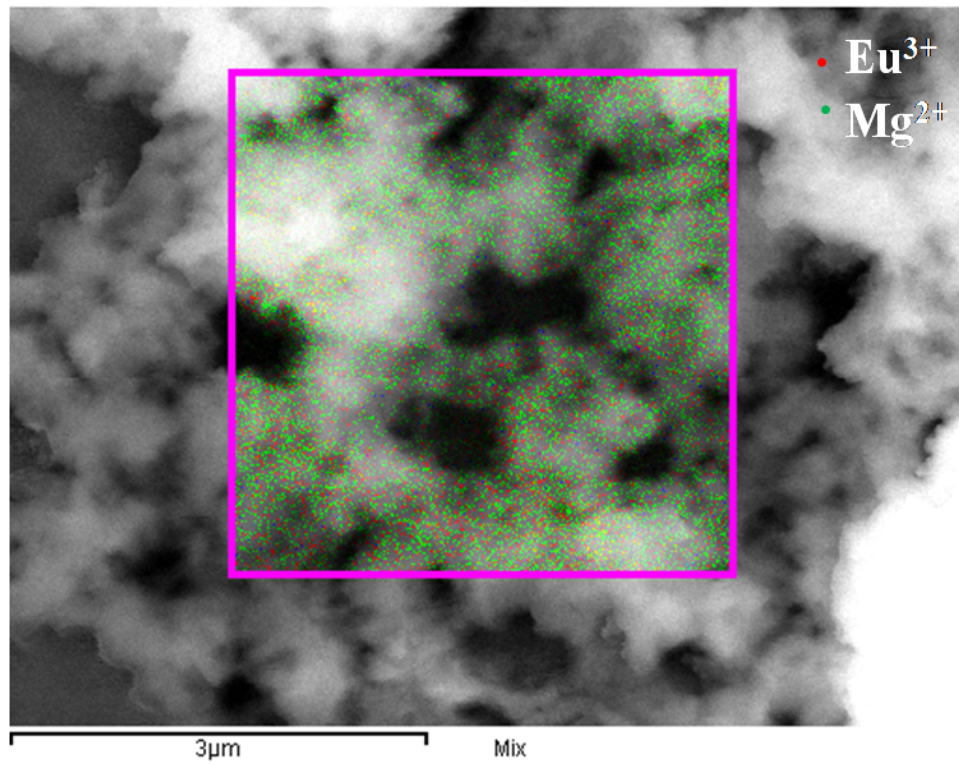


Fig. S6EDAX mapping showing elemental composition for  $\text{Mg}_{1-x}\text{Eu}_x\text{O}:(x/2)\text{V}''_{\text{Mg}}(x=0.01)$  sample

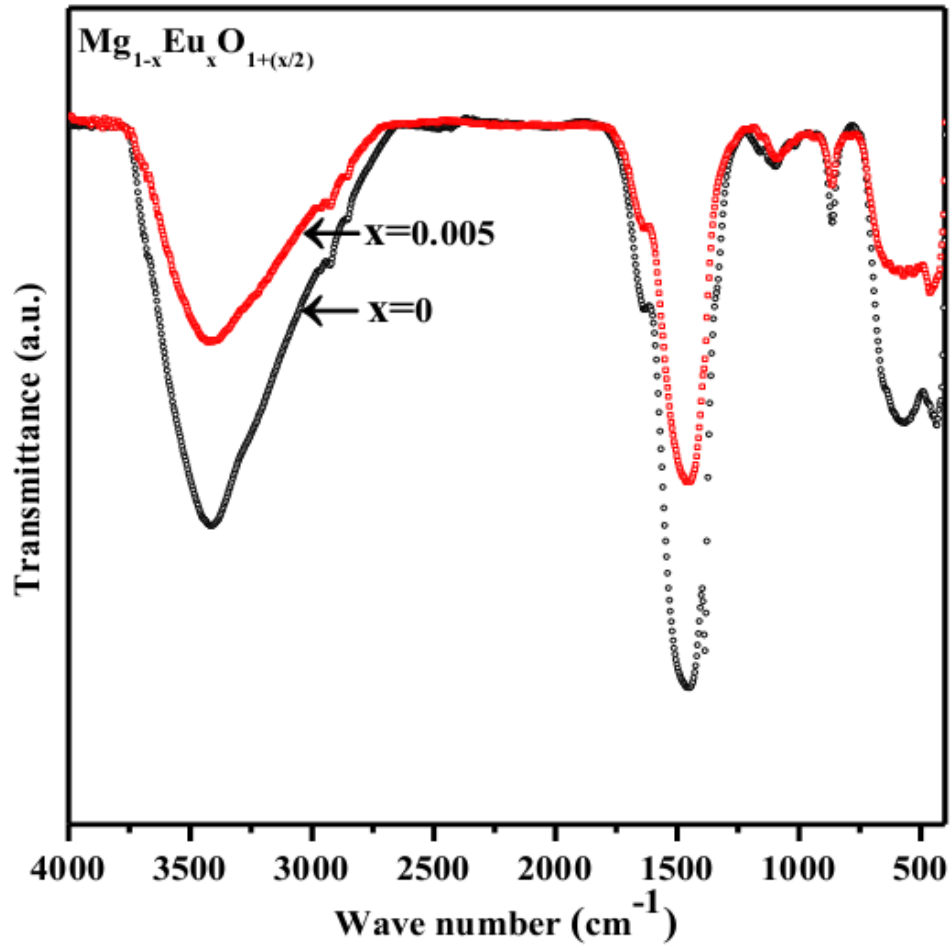


Fig.S7FTIR spectra of MgO and Mg<sub>1-x</sub>Eu<sub>x</sub>O:(x/2)V''<sub>Mg</sub>(x=0.005) samples

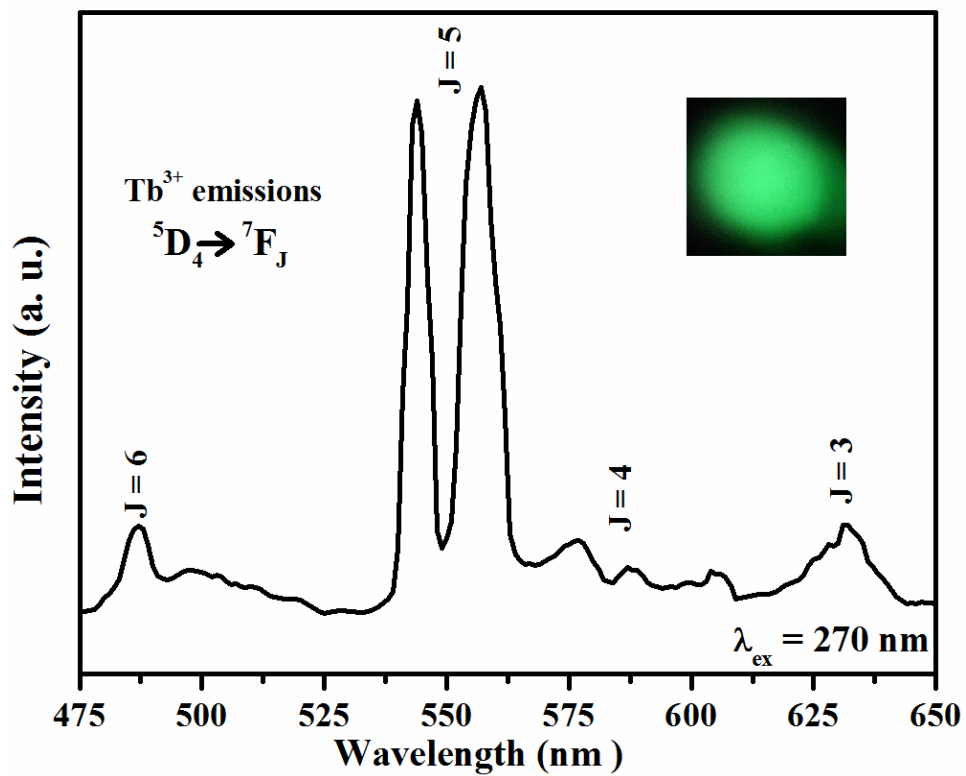


Fig.S8 Emission spectrum of  $\text{Mg}_{1-x}\text{Tb}_x\text{O}:(x/2)\text{V}''_{\text{Mg}}(x=0.005)$  sample upon excitation with 270 nm UV light. A digital photograph of green color emission from  $\text{Mg}_{1-x}\text{Tb}_x\text{O}:(x/2)\text{V}''_{\text{Mg}}(x=0.005)$  sample is also shown in the inset

## REFERENCES

1. P. E. Blochl, *Phys. Rev. B*, 1994, 50, 17953.
2. J. P. Perdew, K. Burke and M. Ernzerhof, *Phys. Rev. Lett.*, 1996, 77, 3865.
3. G. Kresse and D. Joubert, *Phys. Rev. B*, 1999, 59, 1758.
4. G. Kresse and J. Furthmuller, *Phys. Rev. B*, 1996, 54, 11169.
5. R. F. W. Bader, *Chem. Rev.*, 1991, 91, 893.
6. T. Myint, R. Gunawidjaja and H. Eilers, *J. Phys. Chem. C*, 2011, 116, 1687-1693.
7. F. Vetrone, J. C. Boyer, J. A. Capobianco, A. Speghini and M. Bettinelli, *J. Phys. Chem. B*, 2002, 106, 5622-5628.
8. M. L. Debasu, D. Ananias, A. G. Macedo, J. Rocha and L. s. D. Carlos, *J. Phys. Chem. C*, 2011, 115, 15297-15303.
9. H. Guo, N. Dong, M. Yin, W. Zhang, L. Lou and S. Xia, *J. Phys. Chem. B*, 2004, 108, 19205-19209.
10. Y. Liu, W. Luo, R. Li, G. Liu, M. R. Antonio and X. Chen, *J. Phys. Chem. C*, 2008, 112, 686-694.
11. V. A. Fonoberov, K. A. Alim, A. A. Balandin, F. Xiu and J. Liu, *Phys. Rev. B*, 2006, 73, 165317.
12. J. Yang, C. Li, Z. Quan, C. Zhang, P. Yang, Y. Li, C. Yu and J. Lin, *J. Phys. Chem. C*, 2008, 112, 12777-12785.
13. L. Peng, Y. Wang, Z. Wang and Q. Dong, *Appl. Phys. A*, 2011, 102, 387-392.